Title

De novo nonsense mutations in KAT6A, a lysine acetyl-transferase gene, cause a syndrome including microcephaly and global developmental delay.

Journal

American journal of human genetics, 96(3)

ISSN

0002-9297

Authors

Arboleda, Valerie A
Lee, Hane
Dorrani, Naghmeh
et al.

Publication Date

2015-03-01

DOI

10.1016/j.ajhg.2015.01.017

Peer reviewed

REPORT

De Novo Nonsense Mutations in *KAT6A*, a Lysine Acetyl-Transferase Gene, Cause a Syndrome Including Microcephaly and Global Developmental Delay

Valerie A. Arboleda,[1] Hane Lee,[1] Naghmeh Dorrani,[2] Neda Zadeh,[3,4] Mary Willis,[5] Colleen Forsyth Macmurdo,[6] Melanie A. Manning,[6,7] Andrea Kwan,[6,8] Louanne Hudgins,[6] Florian Barthelemy,[9] M. Carrie Miceli,[9] Fabiola Quintero-Rivera,[1] Sibel Kantarci,[1] Samuel P. Strom,[1] Joshua L. Deignan,[1] UCLA Clinical Genomics Center,[1] Wayne W. Grody,[1,2,10] Eric Vilain,[2,10] and Stanley F. Nelson[1,10,*]

Chromatin remodeling through histone acetyltransferase (HAT) and histone deactylase (HDAC) enzymes affects fundamental cellular processes including the cell-cycle, cell differentiation, metabolism, and apoptosis. Nonsense mutations in genes that are involved in histone acetylation and deacetylation result in multiple congenital anomalies with most individuals displaying significant developmental delay, microcephaly and dysmorphism. Here, we report a syndrome caused by de novo heterozygous nonsense mutations in *KAT6A* (a.k.a., MOZ, MYST3) identified by clinical exome sequencing (CES) in four independent families. The same de novo nonsense mutation (c.3385C>T [p.Arg1129*]) was observed in three individuals, and the fourth individual had a nearby de novo nonsense mutation (c.3070C>T [p.Arg1024*]). Neither of these variants was present in 1,815 in-house exomes or in public databases. Common features among all four probands include primary microcephaly, global developmental delay including profound speech delay, and craniofacial dysmorphism, as well as more varied features such as feeding difficulties, cardiac defects, and ocular anomalies. We further demonstrate that *KAT6A* mutations result in dysregulation of H3K9 and H3K18 acetylation and altered P53 signaling. Through histone and non-histone acetylation, KAT6A affects multiple cellular processes and illustrates the complex role of acetylation in regulating development and disease.

Histone-modifying enzymes play key roles in transcriptional regulation and control major cellular processes such as the cell cycle,[1,2] stem cell maintenance, and differentiation.[3,4] These enzymes function within multisubunit protein complexes that target acetyltransferases and deacetylases to specific gene loci to provide cell- and tissue-specific regulation of developmental processes. The combinatorial effects of epigenetic marks influence the accessibility of transcription factor binding sites and can control specific regulatory programs. Epigenetic dysregulation of chromatin is actively studied in both development and cancer and alterations in histone acetylation are implicated in regulating stem cells and differentiation.[5]

In this report, we describe four individual cases in which the presence of de novo mutations suggested that all of them had a previously unrecognized rare autosomal dominant disease. Their syndrome was discovered only after the more routine implementation of clinical exome sequencing (CES) for individuals with potential genetic diseases but without a clear diagnosis.[6,7] All four individuals were sequenced with their parents (trio-CES) to empower the identification of de novo mutations, and all four had de novo nonsense mutations in *KAT6A*. Individuals 1-II-1, 2-II-2 and 3-II-1 underwent trio-CES at the Clinical Genomics Center at UCLA and 4-II-1 underwent trio-CES at GeneDx (Figure 1). CES at UCLA was performed using standard protocols from genomic DNA extraction to data analysis[6,8] in a CLIA-certified laboratory. In these individuals, we identified 21,937 to 23,099 high-quality single nucleotide, insertion, and deletion variants (SNVs and indels) per individual. On the basis of the clinical history of probands 1-II-1, 2-II-2, and 3-II-1, each referring physician generated a list of phenotype keywords that was used to retrieve a primary genelist from the Human Gene Mutation Database (HGMD) and Online Mendelian Inheritance of Man (OMIM). No likely pathogenic variants were identified within any known disease genes in the three individuals sequenced at UCLA. No rare homozygous variants or compound heterozygous variants were identified for recessive disorders, and no variants were identified in known autosomal dominant disorders in any of the individuals. All trio-CES cases are evaluated for potential de novo mutations, and on average each trio-CES case identifies 1.1 de novo, rare, and damaging variants in the

[1]Department of Pathology and Laboratory Medicine, David Geffen School of Medicine, University of California, Los Angeles, Los Angeles, CA 90095, USA; [2]Department of Pediatrics, Division of Medical Genetics, David Geffen School of Medicine, University of California, Los Angeles, Los Angeles, CA 90095, USA, USA; [3]Division of Medical Genetics, CHOC Children's Hospital of Orange County, CA 92868, USA; [4]Genetics Center, Orange, CA 92868, USA; [5]Department of Pediatrics, Naval Medical Center, San Diego, 92134, USA; [6]Department of Pediatrics, Division of Medical Genetics, Stanford University School of Medicine, Stanford, CA 94305, USA; [7]Department of Pathology, Stanford University School of Medicine, Stanford, CA 94305, USA; [8]Department of Genetics, Stanford University School of Medicine, Stanford, CA 94305, USA; [9]Department of Microbiology, Immunology and Molecular Genetics, David Geffen School of Medicine, University of California, Los Angeles, CA 90095, USA; [10]Department of Human Genetics, David Geffen School of Medicine, University of California, Los Angeles, Los Angeles, CA 90095, USA
*Correspondence: snelson@ucla.edu
http://dx.doi.org/10.1016/j.ajhg.2015.01.017.

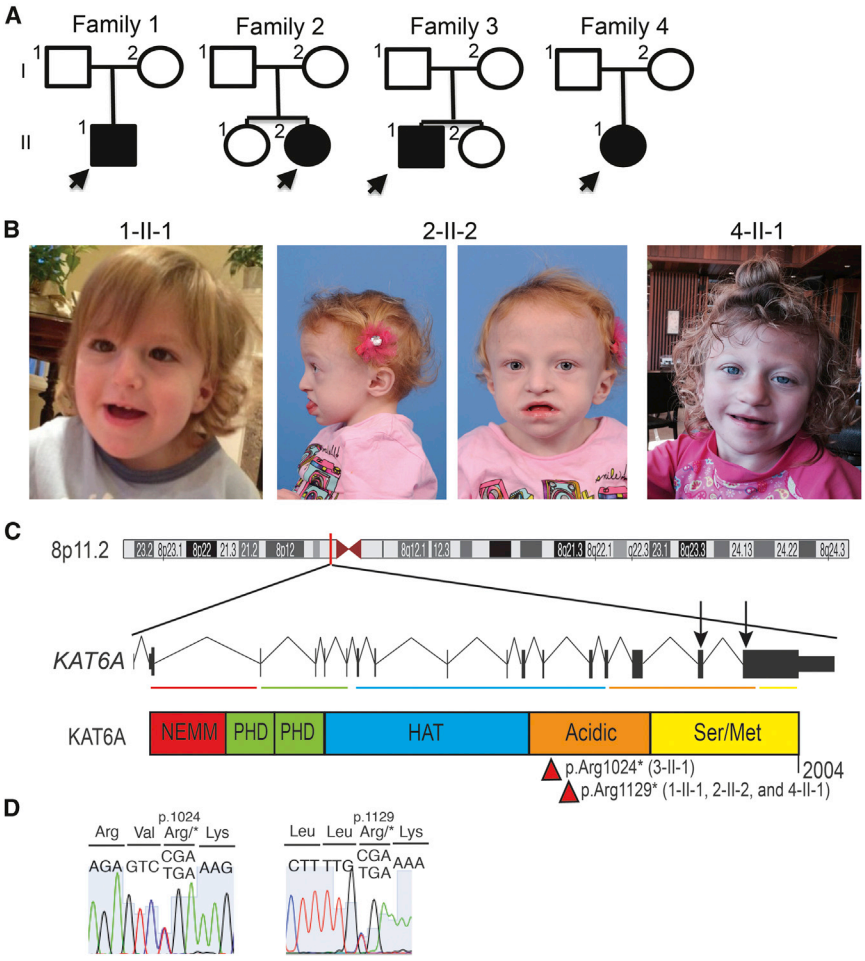

Figure 1. Location of Mutations in *KAT6A*
(A) Pedigrees of families 1–4.
(B) Photos of probands 1-II-1, 2-II-2, and 4-II-1 depict the characteristic eye and nasal features observed in *KAT6A* syndrome.
(C) *KAT6A* is located at 8p11.2. All four de novo mutations are located in exons 16 and 17 (arrows) that are predicted to lead to a truncated protein (red arrowheads) that is missing most of the acidic (orange) and the Serine- and Methionine-rich domains (yellow); NEMM, N-terminal part of Enok, MOZ, or MORF; PHD, Plant homeodomain-linked zinc finger; HAT, Histone Acetyltransferase.
(D) Sequence traces of *KAT6A* from genomic DNA of Proband 1-II-1 demonstrates the p.Arg1129* variant and Proband 3-II-1 demonstrates the p.Arg1024* variant.

proband. In each of the cases presented here, all of them had a de novo mutation in *KAT6A*, and two cases had an additional high-quality de novo variant of uncertain significance in other non-clinical genes.

Because *KAT6A* had not been previously reported in association with a genetic disease, this variant was initially classified in all reports as a variant of uncertain significance.[9] However, three of the four individuals (1-II-1, 2-II-2, and 4-II-1) exhibited the same nucleotide change (c.3385C>T [p.Arg1129*], ClinVarSCV000196747), resulting in a premature stop codon in the terminal exon of *KAT6A*. Individual 3-II-1 had a de novo nonsense variant (c.3070C>T [p.Arg1024*], ClinVarSCV000196748), resulting in a premature stop codon in exon 16 (Table 1, Figure 1). Both transition mutations are at CpG bases. All de novo *KAT6A* mutations identified by the UCLA CGC were confirmed by Sanger sequencing in the proband and his/her parents (Figure 2C), and all mutations are predicted to cause truncation within the acidic domain of the KAT6A protein, leaving the HAT domain intact (Figure 1C).

Within 1,815 clinical exomes sequenced at UCLA, no other nonsense, frameshift, or splice-site variants in *KAT6A* were observed. The missense variant rate estimated from the exome variant server (EVS) data in *KAT6A* is 0.03 (57 rare [<0.1%] variants predicted to be damaging by PolyPhen2 out of 2004 amino acids). This is similar to the missense variant rate of other HAT-encoding genes (*KAT6B*, *CREBBP*, and *EP300)* that are known to cause rare autosomal dominant disorders when mutated and suggests that deleterious missense variations in *KAT6A* are selected against in the human population.

In the Exome Aggregation Consortium (ExAC), which houses nearly 65,000 exomes (including EVS), there are five heterozygous variants (see Table S1) that are predicted to result in a truncated protein and each variant is present in heterozygous form in one individual out of 65,000 exomes. None of the five variants are present in the homozygous form. Two variants are located in intronic regions of the canonical transcript (NM_001099412.1). Of the remaining three variants, variant p.Gln1995* is located ten amino acids from the C terminus and none of the functional domains are disrupted so we predict that the variant is not likely to be pathogenic. However, the remaining two variants p.Ser1113* and p.Ile368_Thr369ins* are located upstream and disrupt multiple known functional protein domains and, based on our cohort, are predicted to be pathogenic. However, these variants are exceedingly rare and without having a complete phenotype from either individual it is unclear whether the individual might be mildly affected with a similar syndrome as described here.

Because the *KAT6A* variants in the three individuals identified through UCLA CES were exceedingly rare, de novo, and deleterious, the clinical histories of the probands were more closely evaluated in order to determine potential overlapping features in their phenotypes. A systematic review of the four children with their treating physicians found several cardinal features present in all three individuals, as well as features that exhibited variable

Table 1. Exome Sequencing Variants

	Total No. Variants (SNVs+ INDELs)[a]	No. Variants MAF < 1%	No. Variants MAF < 1%+AA Changing	No. De Novo Variants[b]	*KAT6A* Variant			
					Genomic Position	cDNA Change	Protein Change	Exon
Proband 1-II-1	21937 (20817+1120)	863	499	2	8:41792353	c.3385C>T	p.Arg1129*	17
Proband 2-II-2	22486 (21145+1341)	949	531	1	8:41792353	c.3385C>T	p.Arg1129*	17
Proband 3-II-1	23099 (21739+1360)	988	571	2	8:41795056	c.3070C>T	p.Arg1024*	16
Proband 4-II-1	Unknown	Unknown	Unknown	1	8:41792353	c.3385C>T	p.Arg1129*	17

MAF, minor allele frequency; AA, amino acid; coding position is on transcript NM_001099412.1.
[a]All variants were submitted to ClinVar under accession codes SCV000196747 and SCV000196748.
[b]Only variants that PASSed after GATK variant recalibration and indel filtration were counted. Only variants that were novel (AF = 0%), amino acid changing in the proband and with QUAL ≥ 500 and coverage ≥ 10× in both the proband and the unaffected parents were counted.

expressivity. Some differences in clinical description were noted between the probands. Clinical features are summarized in Table 2, and the results of genetic, metabolic, and radiographic testing are summarized in Table S2.

Proband 1-II-1 was the first child of non-consanguineous parents conceived through in vitro fertilization. The pregnancy was uncomplicated, with normal screening ultrasounds. He was delivered via cesarean section and at birth was noted to be microcephalic with OccipitalFrontal circumference (OFC) (32 cm, Z = −2.1) but he had a normal weight and length. At 3 months, poor growth was noted with poor swallow function. Nasogastric tube was placed at 8 months followed by gastric tube due to recurrent aspiration pneumonias for which he was hospitalized several times. A large secundum atrial septal defect (ASD) was repaired at age of 5. He had dysmorphic features (Figure 1), brachydactyly, intermittent esotropia, and developmental delay. He was not able to sit independently until 1 year of age and at 3.5 years he remained unable to walk and had absent speech.

Proband 2-II-2 was born at 37 weeks as the second child to non-consanguineous parents. Pregnancy was complicated by preterm labor beginning at 20 weeks and right hydronephrosis diagnosed by fetal ultrasound. Birth weight was normal, but length (45 cm, Z = −3.1) and OFC (34 cm, Z = −2.1) were below the third percentile. At birth she had a cleft palate, intestinal malrotation, ventricular septal defect, bronchomalacia, and esotropia. MRI showed no structural brain defects. Since birth she has been hospitalized numerous times for recurrent urinary tract and respiratory infections. At 9 months, a right pyeloplasty was performed with improvement of recurrent urinary tract infections. At 11 months, cleft palate was repaired and myringotomy tubes were placed for recurrent ear infections. She was diagnosed with autism spectrum disorder at the age of 2 years and received behavioral therapy, which improved behavior, social interactions, and eye contact. Developmentally, she sat independently at 2 years of age and pulled to stand at 2 years 11 months. At the time of last examination at 3 years of age she was non-verbal.

Proband 3-II-1 was born at 42 weeks gestation as the first child of non-consanguineous parents. During the pregnancy, the mother had preterm bleeding and remained on bed rest with suspected placental infarct at 36 weeks. Routine maternal serum screening was normal, and prenatal ultrasounds showed intrauterine growth restriction but were otherwise normal. At birth, weight (1.87 kg, Z = −3.3), length (47.6 cm, Z = −2.6), and head circumference (exact OFC unknown) were less than the third percentile. Postnatally, he had bilateral cryptorchidism, strabismus, feeding difficulty, dysmorphic facial features, and axial hypotonia. He was noted to have global developmental delay without structural neurological defects. He developed a social smile at 3 months, sat independently at 1 year, and walked at 4 years 6 months of age. His height and OFC remained less than the third percentile for age but weight increased appropriately. At 5 years old, he was not communicating verbally.

Proband 4-II-1 was born at 37 weeks to non-consanguineous parents after an uncomplicated pregnancy with normal maternal serum screening and ultrasounds. At birth, she was microcephalic (OFC = 32, Z = −3.0) but with normal weight and length. She was noted to have distinct facial features, ASD, chronic ear infections requiring tympanic tube placement, insomnia-type sleep disturbances, and varying degrees of hypotonia and dystonia. Developmentally, she sat independently by one year of age and by 4.5 years was walking independently but remained without verbal communication.

All four individuals exhibited primary microcephaly with a head circumference less than third percentile (*Z* scores in Table 1), global developmental delay, profound speech delay, and dysmorphic craniofacial features (Figure 1B, Table 2). Photographs of probands from families 1, 3, and 4 were shown to two experienced clinical geneticists and dysmorphologists who noted similar facial features suggestive of disruption of a common developmental pathway. These include a thin upper lip, epicanthal folds, broad nasal bridge, and large forehead. Other medical problems that were present to varying degrees in at least three out of the four children include feeding difficulties, gastric reflux, cardiac septal defects, ocular anomalies, and abnormalities in muscle tone. Many of the features exhibited in these children exist in other well-characterized

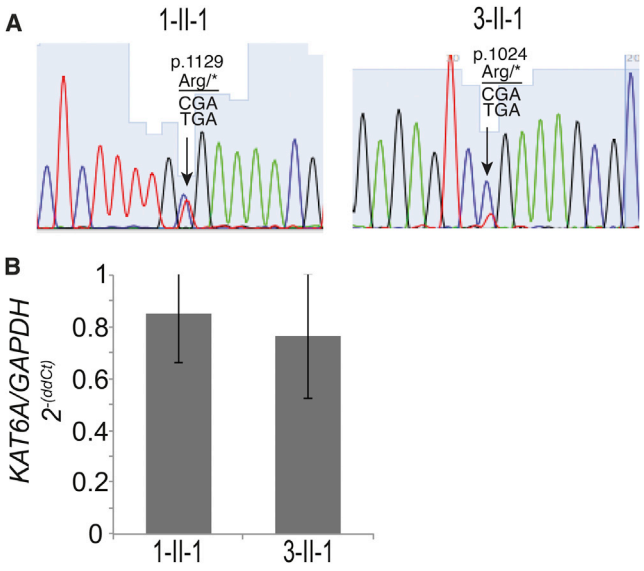

Figure 2. *KAT6A* Mutations Do Not Undergo Nonsense-Mediated Decay

(A) RNA from control (ATCC), proband 1-II-1 and proband 3-II-1 dermal fibroblasts were amplified and sequenced by capillary electrophoresis. The mutation in proband 1-II-1 in the last exon of *KAT6A* showed equal presence of the WT and mutant transcript. The mutation in proband 3-II-1 showed allelic preference for the reference allele.

(B) Quantitative real-time PCR in fibroblasts from proband 1-II-1 and 3-II-1 showed no significant decrease in *KAT6A* mRNA compared to control fibroblast samples. All samples were run triplicate and normalized against *GAPDH*. All samples were compared to biological controls and the ($2^{(-ddCt)}$) method was used for statistical analysis.

genetic[11] syndromes with different genetic etiology, making the recognition of this new syndrome difficult based on phenotype alone. The majority of congenital syndromes have distinctive phenotypes (i.e., genitopatellar syndrome, GPS [MIM606170], in which genital malformations and absent patella are cardinal features) or occur with a relatively high frequency in the general population such as Trisomy 21, Down Syndrome (MIM 190685). In the UCLA CES experience, *KAT6A* de novo mutations have been a common cause of developmental delay, identified in 3/298 CES cases thus far.[6] With increased application of CES to children and undiagnosed adults with developmental delay, mutations in *KAT6A* are likely to be identified in many other children, which will permit better characterization of the phenotypic spectrum affiliated with KAT6A mutations.

In order to understand the molecular mechanisms underlying the phenotype in these children, we obtained dermal fibroblasts from probands 1-II-1 and 3-II-1 and expanded them in culture as in previous studies.[12] All procedures followed were in accordance with the ethical standards of the UCLA IRB and proper informed consent was obtained. To assess the presence of nonsense-mediated decay of the mutant transcript, we sequenced cDNA from fibroblasts to determine whether both the reference and mutant transcript were present from the affected probands 1-II-1 and 3-II-1 (Figure 2A). In 1-II-1, the wild-type (WT) and mutant transcript (c.3385C>T) were present at equal levels. However in 3-II-1, the mutant transcript is decreased there appears to be an allelic imbalance, with less of the mutant transcript compared to the control. Quantitative real-time Taqman PCR for *KAT6A* and *GAPDH* (Life Technologies, 4331182 and 4331182) was performed in triplicate, and no significant decrease in *KAT6A* mRNA transcript was observed between control fibroblasts and those from probands 1-II-1 and 3-II-1 (Figure 2B). Both the normal levels of *KAT6A* mRNA and the equal presence of the WT and mutant transcripts by Sanger sequencing in proband 1-II-1 indicate that mutations in the terminal exon do not result in nonsense-mediated decay.[11] The nonsense variant c.3070C>T is located in the non-terminal exon (as in proband 3-II-1) demonstrates allelic imbalance in favor of the WT allele but without any significant decrease in *KAT6A* transcript levels. Therefore, at basal levels, there is no evidence for substantial nonsense-mediated decay for either *KAT6A* variant. However, we cannot rule out the presence of nonsense-mediated decay or other mechanisms influencing RNA stability when *KAT6A* is upregulated.

KAT6A (a.k.a., *MYST3*, *MOZ)* is a lysine (K) acetyltransferase that is located on chromosome 8p11.2 and is a member of the MYST family of proteins. All members of the MYST family contain a highly conserved catalytic histone acetyl transferase (HAT) domain with roles in both histone lysine acetylation[13] and protein lysine acetylation.[14,15] *KAT6A* was originally identified as a recurrent translocation t(8;16)(p11;p13) in acute monocytic leukemia.[16] Since then, recurrent translocations of *KAT6A* with *CREBBP*,[17] *EP300*,[18] and *TIF2*[19] have been identified in a subset of individuals diagnosed with myeloid malignancies who are refractory to chemotherapy. Additional studies have shown that histone acetylation by KAT6A regulates *Hox* gene expression in human umbilical cord blood stem cells[20] and mouse craniofacial development[21] and controls *Tbx1* expression in mouse cardiogenesis. Mutations in *KAT6A* have never been associated with a constitutional genetic syndrome.

Functionally, *KAT6A* has important roles in gene-specific histone 3 acetylation[22] regulating developmental gene expression[21,23] and in P53 acetylation and signaling.[15] Both histone acetylation and p53 pathways have been previously shown to control a wide range of processes such as DNA repair and replication, metabolism, cell mobility, stem cell maintenance,[24] and senescence.[25–27] To test whether global histone acetylation patterns were perturbed by *KAT6A* mutations, we performed histone extraction[28] on control fibroblasts (ATCC) and dermal fibroblasts from proband 1-II-1. Histone extractions were subject to Western blot and probed using antibodies to core histone 3 and specific acetylated forms of histone 3 as follows: H3K9, H3K14, H3K18, H3K27, and H3K56 (Acetyl-Histone H3 Antibody Kit, Cell Signaling 9927), core histones 2A, 2B, and 4 and acetylated H2AK5, H2BK5 and H4K8

Table 2. Common Clinical Features in Individuals with Nonsense Mutations in *KAT6A*

		1-II-1	2-II-2	3-II-1	4-II-1
Karyotype		46,XY	46,XX	46,XY	46,XX
Age at last examination		3 years 3 months	2 years 11 months	5 years	4 years
Neurological					
Microcephaly cm (Z-score)	Birth:	32.8 (−2.1)	34.0(−2.1)	unknown	32.0(−3.0)
	Last Exam	47(−2.33)	45.8(−2.78)	48.0(−2.52) at 4.5 years	46.5(−2.81)
Length/Height cm (Z-score)	Birth:	48.3(−1.7)	45(−3.1)	47.6 (−2.0)	unknown
	Last Exam	92.8(−1.1)	84.3(−2.6)	97.0(−2.6) at 4.5 years	98.9(−1.4)
Weight kg (Z-score)	Birth	3.08(−1.3)	2.8(−1.8)	1.87 (−3.3)	2.95(−1.5)
	Last Exam	14.85(0)	10.4(−2.86)	16.92 (−0.7) 4.5 years	14.6(−1.3)
Developmental Delay (Gross motor)		Pull to stand at 2.5 years	Rolling over: 4 mo, Sat unassisted: 1yr, Pull to stand at 2.9 years	Sat unassisted: 1 year, walked:4.5 years	Sat unassisted:1 year, Pull to stand: 1.5 years
Intellectual disability		Absent speech, no words	Absent speech, no words	Absent speech, no words	Absent speech, no words
Social/Emotional development		Social smile at 4 months	Social smile at 3 months	Social smile at 3 months	Social smile at 3 months
Disturbances in sleep behavior		sleep apnea	NE	NE	sleep disorder-insomnia type
Facial					
Nasal anomalies		Prominent bridge, full nasal tip	Prominent root	short nose, bifid tip	lateral nasal build-up
Cleft palate		−	+	−	−
Dental anomalies		−	+	+	−
Other		Rosebud mouth	Large upper canines	Lower teeth are small and peg-shaped	−
Ocular					
Strabismus		+	+	+	−
Epicanthal fold		+ (left)	−	+ (bilateral)	−
Optic Nerve Atrophy		NE	NE	+	−
Ptosis		−	−	+	+ (left only)
Myopia		−	−	−	+
Cardiac					
ASD		+	−	NE	+
VSD		−	+	NE	−
Pulmonary					
Broncho- or laryngomalacia		+	−	−	−
Chronic Lung Disease		+	+	−	−
Gastrointestinal					
Reflux		+	+	+	−
Feeding Difficulty		+ [a]	+ [a]	+	−
Intestinal Malrotation		−	+	−	−
Genitourinary					
Hydronephrosis		−	+	−	−
Cryptorchidism		−	NA	+	NA

(*Continued on next page*)

Table 2. ***Continued***

	1-II-1	2-II-2	3-II-1	4-II-1
Hypospadias	–	–	–	–
Musculoskeletal				
Hypotonia	+	–	+ (axial)	+
Brachydactyly	middle finger/total hand length: 25th percentile, overlapping toes 2nd over 3rd	–	Brachydactyly	–
Dystonia	+	–	–	+
Other		L. hand flexed PIP	prenatal growth restriction	

NE, not evaluated; ASD, atrial septal defect; VSD, ventricular septal defect.
[a]With gastrointestinal tube dependence. For weight and length/height, *Z* scores were calculated using the CDC charts for children ages 2–20. Head circumference at birth was calculated using CDC charts for infants. For head circumference in children older than 2, *Z* score was calculated based on published data.[10]

(Acetyl-Histone Antibody Sampler Kit, Cell Signaling 9933). All experiments were performed in duplicate. We observed a decrease in H3K9 acetylation and increase in H3K18 acetylation in Proband 1-II-1 fibroblasts compared to the control fibroblasts (Figure 3A). No histone acetylation was observed in H3K14, H3K27, H3K56, H2AK5, and H2BK5 in either cell type, and no change in histone acetylation was observed in H4K8 (data not shown).

KAT6A acetylation of P53 has also been shown to regulate downstream P53 signaling.[15] KAT6A acetylates residues K382 and K120 on P53[15] in vivo and deletion constructs demonstrated the requirement for both the HAT domain and the Serine and Methionine (SM) rich domain for interaction with P53. Therefore, we hypothesized that the truncation of the C terminus of KAT6A results in loss of the SM domain leading to decreased P53 acetylation and dysregulation of downstream P53 signaling. We generated RNA sequencing libraries using Illumina TruSeq RNA sample prep V2 in duplicate, and libraries were pooled and sequenced on Illumina HiSeq (UCLA Clinical Microarray Core). All reads were aligned with the STAR aligner[29] and processed using Cufflinks.[29,30] Because KAT6A is known to be involved in P53 signaling, we examined 92 genes involved in P53 signaling. We did not observe any significant changes in *TP53* mRNA levels. However, 30 genes showed significant changes in gene expression between control fibroblasts and fibroblasts from either 1-II-1 or 3-II-1(Figure 3B), based on the q value less than the determined false discovery rate. These genes were analyzed through David Functional Annotation Resource[31,32] and showed significant enrichment for genes important in apoptosis ($p < 10^{-5}$), nuclear transcriptional regulation ($p < 10^{-5}$), and cellular metabolism ($p < 10^{-5}$). Results from all genes are in Figure S1 and Table S4. During development the truncated KAT6A protein exerts its damaging effect on organogenesis through dysregulated chromatin modification and P53 signaling.

Mouse models with homozygous deletion of *Kat6a* are lethal during embryogenesis or in the perinatal period due to vascular and cardiac anomalies. *Kat6a*$^{-/-}$ mice have abnormalities in the gastrointestinal tract, cardiac defects, thymic hypoplasia, splenic hypoplasia,[33] skeletal anomalies,[21] decreased neural[34] and hematopoietic stem cell,[35] and improper B cell differentiation.[36] Similar to the clinical phenotype, there are no structural brain anomalies in *Kat6a*$^{-/-}$ mice. The loss of hematopoietic stem cells seen in mice is due to specific disruption of the catalytic HAT domain with maintenance of the transcriptional activation and repression domains at the N and C termini of Kat6a.[34,36] To date, the children with *KAT6A* mutations described here do not have any defects in hematopoiesis indicating that either a single copy of WT *KAT6A* or that together the WT and truncated alleles are sufficient to maintain hematopoiesis. However, based on the observations in the mice, these children might experience hematological or immunological problems with time, and it would be clinically prudent to continually monitor these individuals with mutations in for evidence of hematopoietic defects.

Nonsense or frameshift truncating de novo mutations in a highly homologous member of the MYST family, *KAT6B* (a.k.a. *MYST4, MORF*) have recently been described as the etiology of GPS (MIM 606170)[37,38] and Say-Barber-Biesecker-Young-Simpson Variant of Ohdo syndrome (SBBVYS [MIM 603736]).[39,40] However, the distinctive phenotypes between both syndromes are derived from a predicted differential effect of the multiple functional protein domains. The common features between GPS and SBBVYS might be due to a common loss of function of the C-terminal domains,[40] whereas phenotypes that distinguish them are hypothesized to result from expression of the truncated protein in GPS with potential gain-of-function effects.[40] Within our cohort of de novo mutations in *KAT6A*, we observe that proband 3-II-1 who has the p.Arg1024* variant had significant intrauterine growth retardation that was not seen in the children with the p.Arg1129* variant. We hypothesize that the differential phenotype might result from the allelic imbalance seen in the p.Arg1024* fibroblasts or secondary to effects of KAT6A targeting by the C-terminal domain. However, even among

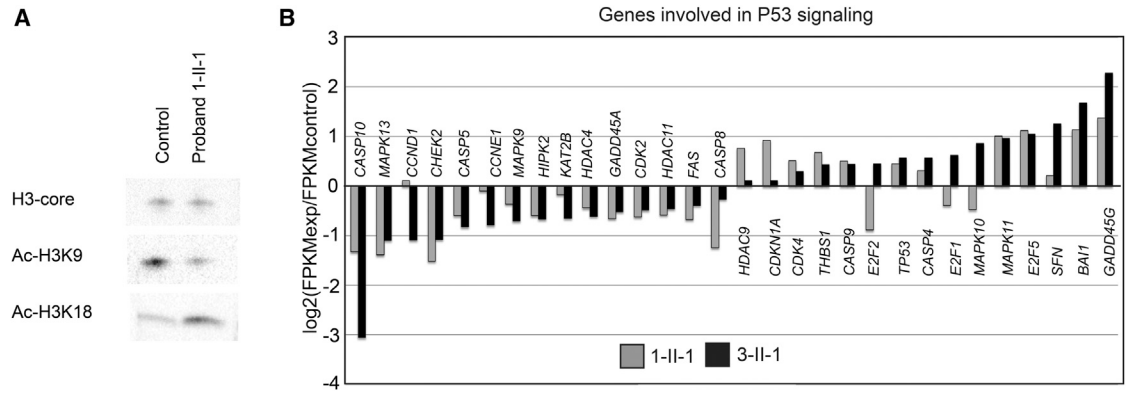

Figure 3. *KAT6A* Nonsense Mutations Result in Global Changes in Histone Acetylation and p53 Signaling Pathways
(A) H3K9 acetylation was decreased in histone extracts from proband 1-II-1 dermal fibroblasts relative to control. H3K18 acetylation was increased in proband 1-II-1 dermal fibroblasts compared to control. All experiments were performed in duplicate.
(B) Genes in the P53 signaling pathway that show significant differences between experimental (Proband 1-II-1 or Proband 3-II-1) and control fibroblasts growing in culture were assessed using RNaseq. All genes shown were significantly increased or decreased if the q value was less than the FDR-adjusted p value of the test statistic.

the individuals with identical *KAT6A* genotype, there is significant variability in the phenotype of individuals which further points to the importance of genetic background and environment in determining the phenotypic expression of the mutation.

Beyond syndromes caused by mutations in genes encoding the MYST family of histone acetyltranferases, we reviewed genetic syndromes caused by genes that have histone acetyltransferase or deacetylase function. The major commonalities between these syndromes are microcephaly (not reported with mutations in *IKBKAP* or *HDAC6*), global developmental delay, craniofacial dysmorphism, and limb anomalies. Individuals with mutations in acetyltransferase genes more commonly display multi-organ defects, such as congenital heart disease, feeding difficulties, lung disease, and hypotonia, whereas these are less frequently observed in individuals with HDAC mutations. Individuals with mutations in HDAC genes were more likely to experience significant growth retardation and truncal obesity compared to mutations in histone acetyltransferase genes.

Given the high prevalence of mutations in *KAT6A* identified in our cohort of exome sequencing cases with developmental delay, we screened all individuals who underwent UCLA CES for developmental delay (n = 298) for de novo mutations in 35 genes encoding histone acetyltransferases and deacetylases (Table S3). A total of 8 de novo mutations were identified in genes that modify histone acetyl groups. Causative mutations were identified in the clinical genes *KAT6B*, *CREBBP*, *HDAC8*, and *EP300* (reported in [6]). At UCLA, four de novo mutations were identified in *KAT6A*, three reported here and a fourth de novo missense mutation in *KAT6A* that was identified in a child for whom CES was performed at UCLA with pontocerebellar hypoplasia.[6] However, an alternate mutation in *CASK* was also identified in that case and reported as more likely to be causal of the child's phenotype. It is possible that *KAT6A* missense variants could be a modifier of mutations in other genes. Thus, in our cases of developmental delay, we have observed three cases with de novo nonsense mutations, making the frequency of *KAT6A* mutations one percent (3/298) of all cases of developmental delay referred for clinical exome sequencing.

In line with the known role of KAT6A in histone acetylation, it is tempting to speculate that drug therapies might restore a more normal acetylation profile and reduce the developmental delay in individuals with *KAT6A* mutations. Drugs that inhibit HDAC activity are actively being studied as therapeutics in cancer,[41] neurodegenerative disorders such as Parkinson and Alzheimer disease,[41] muscular dystrophies,[42,43] and to modulate developmental delay caused by mutations in histone acetyltransferase genes *CRBBP* and *EP300*.[44–46] However, much work needs to be done to understand complex the molecular pathways that are perturbed in individuals with *KAT6A* mutations and how they affect critical cellular processes in development and beyond.

In conclusion, we have identified *KAT6A* mutations as a frequent cause of syndromic developmental delay with microcephaly and dysmorphic features. Given the incredible rarity of most genetic syndromes, the fact that three cases had been identified at UCLA out of the first 298 CES cases performed for developmental delay makes *KAT6A* syndrome one of the more common causes of syndromic developmental delay. Our data demonstrates that the mutant *KAT6A* allele alters global acetylation of H3K9 and H3K18 and affects P53-mediated pathways in apoptosis, metabolism, and transcriptional regulation.

Accession Numbers

The ClinVar accession numbers for the *KAT6A* sequence reported in this paper are SCV000196747 and SCV000196748.

Supplemental Data

Supplemental Data include one figure and four tables and can be found with this article online at http://dx.doi.org/10.1016/j.ajhg.2015.01.017.

Acknowledgments

We thank the all the families for participating in the study. Individuals who are interested in connecting with other families with KAT6A can find more information at http://www.chloekat6a.org/. Expansion of the cell lines was supported by NIH/National Institute of Arthritis Musculoskeletal and Skin (NIAMS) NIH-P30-5P30AR057230. NIH/National Center for Advancing Translational Science (NCATS) UCLA CTSI UL1TR000124 provided support for cores. The authors would like to thank the Exome Aggregation Consortium and the groups that provided exome variant data for comparison. A full list of contributing groups can be found at http://exac.broadinstitute.org/about. The views expressed in this article are the authors' and do not necessarily reflect the official policy or position of the Department of the Navy, Department of Defense, or the U.S. Government. Partial support for this project was provided by UCLA Translational Pathology Research Fund grant to V.A.A., S.F.N., and H.L.

Received: October 20, 2014
Accepted: January 20, 2015
Published: February 26, 2015

Web Resources

The URLs for data presented herein are as follows:

ClinVar, https://www.ncbi.nlm.nih.gov/clinvar/
ExAC Browser, http://exac.broadinstitute.org/
NHLBI Exome Sequencing Project (ESP) Exome Variant Server, http://evs.gs.washington.edu/EVS/
OMIM, http://www.omim.org/

References

1. Doenecke, D. (2014). Chromatin dynamics from S-phase to mitosis: contributions of histone modifications. Cell Tissue Res. *356*, 467–475.
2. Kim, W., Choi, M., and Kim, J.E. (2014). The histone methyltransferase Dot1/DOT1L as a critical regulator of the cell cycle. Cell Cycle *13*, 726–738.
3. McGann, J.C., Oyer, J.A., Garg, S., Yao, H., Liu, J., Feng, X., Liao, L., Yates, J.R., 3rd, and Mandel, G. (2014). Polycomb- and REST-associated histone deacetylases are independent pathways toward a mature neuronal phenotype. eLife *3*, e04235.
4. Leung, K.S., Cheng, V.W., Mok, S.W., and Tsui, S.K. (2014). The involvement of DNA methylation and histone modification on the epigenetic regulation of embryonic stem cells and induced pluripotent stem cells. Curr. Stem Cell Res. Ther. *9*, 388–395.
5. Yang, X.J., and Ullah, M. (2007). MOZ and MORF, two large MYSTic HATs in normal and cancer stem cells. Oncogene *26*, 5408–5419.
6. Lee, H., Deignan, J.L., Dorrani, N., Strom, S.P., Kantarci, S., Quintero-Rivera, F., Das, K., Toy, T., Harry, B., Yourshaw, M., et al. (2014). Clinical exome sequencing for genetic identification of rare Mendelian disorders. JAMA *312*, 1880–1887.
7. Yang, Y., Muzny, D.M., Reid, J.G., Bainbridge, M.N., Willis, A., Ward, P.A., Braxton, A., Beuten, J., Xia, F., Niu, Z., et al. (2013). Clinical whole-exome sequencing for the diagnosis of mendelian disorders. N. Engl. J. Med. *369*, 1502–1511.
8. Rehm, H.L., Bale, S.J., Bayrak-Toydemir, P., Berg, J.S., Brown, K.K., Deignan, J.L., Friez, M.J., Funke, B.H., Hegde, M.R., Lyon, E., et al. (2013). ACMG clinical laboratory standards for next-generation sequencing. Genetics in medicine: official journal of the American College of Medical Genetics *15*, 733–747.
9. Duzkale, H., Shen, J., McLaughlin, H., Alfares, A., Kelly, M.A., Pugh, T.J., Funke, B.H., Rehm, H.L., and Lebo, M.S. (2013). A systematic approach to assessing the clinical significance of genetic variants. Clin. Genet. *84*, 453–463.
10. Rollins, J.D., Collins, J.S., and Holden, K.R. (2010). United States head circumference growth reference charts: birth to 21 years. The Journal of pediatrics *156*, 907–913, 913 e901-902.
11. Fang, Y., Bateman, J.F., Mercer, J.F., and Lamandé, S.R. (2013). Nonsense-mediated mRNA decay of collagen -emerging complexity in RNA surveillance mechanisms. J. Cell Sci. *126*, 2551–2560.
12. Lowry, W.E., Richter, L., Yachechko, R., Pyle, A.D., Tchieu, J., Sridharan, R., Clark, A.T., and Plath, K. (2008). Generation of human induced pluripotent stem cells from dermal fibroblasts. Proc. Natl. Acad. Sci. USA *105*, 2883–2888.
13. Champagne, N., Pelletier, N., and Yang, X.J. (2001). The monocytic leukemia zinc finger protein MOZ is a histone acetyltransferase. Oncogene *20*, 404–409.
14. Sapountzi, V., and Côté, J. (2011). MYST-family histone acetyltransferases: beyond chromatin. Cell. Mol. Life Sci. *68*, 1147–1156.
15. Rokudai, S., Laptenko, O., Arnal, S.M., Taya, Y., Kitabayashi, I., and Prives, C. (2013). MOZ increases p53 acetylation and premature senescence through its complex formation with PML. Proc. Natl. Acad. Sci. USA *110*, 3895–3900.
16. Borrow, J., Stanton, V.P., Jr., Andresen, J.M., Becher, R., Behm, F.G., Chaganti, R.S., Civin, C.I., Disteche, C., Dubé, I., Frischauf, A.M., et al. (1996). The translocation t(8;16)(p11;p13) of acute myeloid leukaemia fuses a putative acetyltransferase to the CREB-binding protein. Nat. Genet. *14*, 33–41.
17. Kitabayashi, I., Aikawa, Y., Nguyen, L.A., Yokoyama, A., and Ohki, M. (2001). Activation of AML1-mediated transcription by MOZ and inhibition by the MOZ-CBP fusion protein. EMBO J. *20*, 7184–7196.
18. Chaffanet, M., Gressin, L., Preudhomme, C., Soenen-Cornu, V., Birnbaum, D., and Pébusque, M.J. (2000). MOZ is fused to p300 in an acute monocytic leukemia with t(8;22). Genes Chromosomes Cancer *28*, 138–144.
19. Carapeti, M., Aguiar, R.C., Goldman, J.M., and Cross, N.C. (1998). A novel fusion between MOZ and the nuclear receptor coactivator TIF2 in acute myeloid leukemia. Blood *91*, 3127–3133.
20. Hibiya, K., Katsumoto, T., Kondo, T., Kitabayashi, I., and Kudo, A. (2009). Brpf1, a subunit of the MOZ histone acetyl transferase complex, maintains expression of anterior and posterior Hox genes for proper patterning of craniofacial and caudal skeletons. Dev. Biol. *329*, 176–190.
21. Voss, A.K., Collin, C., Dixon, M.P., and Thomas, T. (2009). Moz and retinoic acid coordinately regulate H3K9 acetylation, Hox gene expression, and segment identity. Dev. Cell *17*, 674–686.

22. Ali, M., Yan, K., Lalonde, M.E., Degerny, C., Rothbart, S.B., Strahl, B.D., Côté, J., Yang, X.J., and Kutateladze, T.G. (2012). Tandem PHD fingers of MORF/MOZ acetyltransferases display selectivity for acetylated histone H3 and are required for the association with chromatin. J. Mol. Biol. *424*, 328–338.
23. Kong, Y., Grimaldi, M., Curtin, E., Dougherty, M., Kaufman, C., White, R.M., Zon, L.I., and Liao, E.C. (2014). Neural crest development and craniofacial morphogenesis is coordinated by nitric oxide and histone acetylation. Chem. Biol. *21*, 488–501.
24. Perez-Campo, F.M., Costa, G., Lie-A-Ling, M., Stifani, S., Kouskoff, V., and Lacaud, G. (2014). MOZ-mediated repression of p16(INK) (4) (a) is critical for the self-renewal of neural and hematopoietic stem cells. Stem Cells *32*, 1591–1601.
25. Rokudai, S., Aikawa, Y., Tagata, Y., Tsuchida, N., Taya, Y., and Kitabayashi, I. (2009). Monocytic leukemia zinc finger (MOZ) interacts with p53 to induce p21 expression and cell-cycle arrest. J. Biol. Chem. *284*, 237–244.
26. Wang, Y.V., Leblanc, M., Fox, N., Mao, J.H., Tinkum, K.L., Krummel, K., Engle, D., Piwnica-Worms, D., Piwnica-Worms, H., Balmain, A., et al. (2011). Fine-tuning p53 activity through C-terminal modification significantly contributes to HSC homeostasis and mouse radiosensitivity. Genes Dev. *25*, 1426–1438.
27. Vousden, K.H., and Prives, C. (2009). Blinded by the Light: The Growing Complexity of p53. Cell *137*, 413–431.
28. Murray, K. (1966). The acid extraction of histones from calf thymus deoxyribonucleoprotein. J. Mol. Biol. *15*, 409–419.
29. Dobin, A., Davis, C.A., Schlesinger, F., Drenkow, J., Zaleski, C., Jha, S., Batut, P., Chaisson, M., and Gingeras, T.R. (2013). STAR: ultrafast universal RNA-seq aligner. Bioinformatics *29*, 15–21.
30. Trapnell, C., Roberts, A., Goff, L., Pertea, G., Kim, D., Kelley, D.R., Pimentel, H., Salzberg, S.L., Rinn, J.L., and Pachter, L. (2012). Differential gene and transcript expression analysis of RNA-seq experiments with TopHat and Cufflinks. Nat. Protoc. *7*, 562–578.
31. Huang, W., Sherman, B.T., and Lempicki, R.A. (2009). Systematic and integrative analysis of large gene lists using DAVID bioinformatics resources. Nat. Protoc. *4*, 44–57.
32. Huang, W., Sherman, B.T., and Lempicki, R.A. (2009). Bioinformatics enrichment tools: paths toward the comprehensive functional analysis of large gene lists. Nucleic Acids Res. *37*, 1–13.
33. Voss, A.K., Vanyai, H.K., Collin, C., Dixon, M.P., McLennan, T.J., Sheikh, B.N., Scambler, P., and Thomas, T. (2012). MOZ regulates the Tbx1 locus, and Moz mutation partially phenocopies DiGeorge syndrome. Dev. Cell *23*, 652–663.
34. Perez-Campo, F.M., Borrow, J., Kouskoff, V., and Lacaud, G. (2009). The histone acetyl transferase activity of monocytic leukemia zinc finger is critical for the proliferation of hematopoietic precursors. Blood *113*, 4866–4874.
35. Thomas, T., Corcoran, L.M., Gugasyan, R., Dixon, M.P., Brodnicki, T., Nutt, S.L., Metcalf, D., and Voss, A.K. (2006). Monocytic leukemia zinc finger protein is essential for the development of long-term reconstituting hematopoietic stem cells. Genes Dev. *20*, 1175–1186.
36. Good-Jacobson, K.L., Chen, Y., Voss, A.K., Smyth, G.K., Thomas, T., and Tarlinton, D. (2014). Regulation of germinal center responses and B-cell memory by the chromatin modifier MOZ. Proc. Natl. Acad. Sci. USA *111*, 9585–9590.
37. Campeau, P.M., Kim, J.C., Lu, J.T., Schwartzentruber, J.A., Abdul-Rahman, O.A., Schlaubitz, S., Murdock, D.M., Jiang, M.M., Lammer, E.J., Enns, G.M., et al. (2012). Mutations in KAT6B, encoding a histone acetyltransferase, cause Genitopatellar syndrome. Am. J. Hum. Genet. *90*, 282–289.
38. Simpson, M.A., Deshpande, C., Dafou, D., Vissers, L.E., Woollard, W.J., Holder, S.E., Gillessen-Kaesbach, G., Derks, R., White, S.M., Cohen-Snuijf, R., et al. (2012). De novo mutations of the gene encoding the histone acetyltransferase KAT6B cause Genitopatellar syndrome. Am. J. Hum. Genet. *90*, 290–294.
39. Clayton-Smith, J., O'Sullivan, J., Daly, S., Bhaskar, S., Day, R., Anderson, B., Voss, A.K., Thomas, T., Biesecker, L.G., Smith, P., et al. (2011). Whole-exome-sequencing identifies mutations in histone acetyltransferase gene KAT6B in individuals with the Say-Barber-Biesecker variant of Ohdo syndrome. Am. J. Hum. Genet. *89*, 675–681.
40. Campeau, P.M., Lu, J.T., Dawson, B.C., Fokkema, I.F., Robertson, S.P., Gibbs, R.A., and Lee, B.H. (2012). The KAT6B-related disorders genitopatellar syndrome and Ohdo/SBBYS syndrome have distinct clinical features reflecting distinct molecular mechanisms. Hum. Mutat. *33*, 1520–1525.
41. Falkenberg, K.J., and Johnstone, R.W. (2014). Histone deacetylases and their inhibitors in cancer, neurological diseases and immune disorders. Nat. Rev. Drug Discov. *13*, 673–691.
42. Consalvi, S., Mozzetta, C., Bettica, P., Germani, M., Fiorentini, F., Del Bene, F., Rocchetti, M., Leoni, F., Monzani, V., Mascagni, P., et al. (2013). Preclinical studies in the mdx mouse model of duchenne muscular dystrophy with the histone deacetylase inhibitor givinostat. Mol. Med. *19*, 79–87.
43. Colussi, C., Gurtner, A., Rosati, J., Illi, B., Ragone, G., Piaggio, G., Moggio, M., Lamperti, C., D'Angelo, G., Clementi, E., et al. (2009). Nitric oxide deficiency determines global chromatin changes in Duchenne muscular dystrophy. FASEB journal: official publication of the Federation of American Societies for Experimental Biology *23*, 2131–2141.
44. Mahgoub, M., and Monteggia, L.M. (2014). A role for histone deacetylases in the cellular and behavioral mechanisms underlying learning and memory. Learn. Mem. *21*, 564–568.
45. Barrett, R.M., and Wood, M.A. (2008). Beyond transcription factors: the role of chromatin modifying enzymes in regulating transcription required for memory. Learn. Mem. *15*, 460–467.
46. Alarcón, J.M., Malleret, G., Touzani, K., Vronskaya, S., Ishii, S., Kandel, E.R., and Barco, A. (2004). Chromatin acetylation, memory, and LTP are impaired in CBP+/- mice: a model for the cognitive deficit in Rubinstein-Taybi syndrome and its amelioration. Neuron *42*, 947–959.